Energy, Environmental, and Catalysis Applications

Highly adsorptive and magneto-inductive Guefoams (multifunctional guest-containing foams) for enhanced energy-efficient preconcentration and management of VOCs

José Miguel Miguel Molina Jordá

ACS Appl. Mater. Interfaces, **Just Accepted Manuscript** • DOI: 10.1021/acsami.9b22858 • Publication Date (Web): 18 Feb 2020

Highly adsorptive and magneto-inductive Guefoams (multifunctional guest-containing foams) for enhanced energy-efficient preconcentration and management of VOCs

J.M. Molina-Jordá *

Department of Inorganic Chemistry, University of Alicante, Ap. 99, E-03080 Alicante, Spain

University Materials Institute of Alicante, University of Alicante, Ap. 99, E-03080 Alicante, Spain

Keywords: multifunctional; guest; host; adsorption; magnetic induction; open-pore foam, preconcentration, volatile organic compounds (VOCs).

* corresponding author: jmmj@ua.es

Abstract

The design of multifunctional materials is a current demand for high-end technological applications that need to combine different functions unable to be accomplished by a single material. The aim of this work is to present, at first glance, a new family of recently patented multifunctional porous materials developed by locating granular phases with specific functionality (guests) within the cavities of open-pore cellular materials (hosts) and, at second glance, the use of a set of these materials for the preconcentration and management of volatile organic compounds (VOCs). These materials (herein known as Guefoams, acronym for Guest-containing foams), present host foams and guest phases that are not bonded and therefore allow fluids to pass through. The processing method is the gas pressure infiltration of a host precursor into

preforms containing particulate guest phases covered by a NaCl martyr coating, which is later dissolved in water. The manuscript shows the manufacture and characterization of a specific set of Guefoams composed of aluminum foams that incorporate both steel particles and activated carbon particles as guest phases into the same material. These guest phases make the materials highly adsorbent and susceptible to rapid desorption by magnetic induction, two properties never achieved with traditional foams that transform these materials into perfect candidates for preconcentration and energy-efficient management of VOCs. The manuscript concludes with a discussion on advisable properties to consider when exploring the use of these materials in the mentioned applications.

1. Introduction

Integrating different, even contradictory or excluding functions into the same material system is now a fundamental challenge that constitutes an interesting perspective for many modern applications, seeking to improve the quality of human life and address global challenges [1,2]. Given their wide variety of potential applications in recent years, these so-called multifunctional materials have aroused great interest in the scientific community. Multifunctional materials are often formed by a combination of materials (multimaterials), each with one or more functionalities following a characteristic design. Knowledge of the individual functions of materials themselves is sometimes insufficient to predict the behavior of multimaterials in a given application as their final properties emerge from the symbiosis of constituent material properties. Designing and manufacturing new multifunctional multimaterials is one of the most promising research lines in the coming years.

This paper presents a new family of multifunctional materials that represent a promising generation of porous materials with expanded functionalities. The original idea behind these materials is to extend the limited functions of traditional foams, the properties of which are normally limited by the nature of the material as well as by the shape, geometry and pore size distribution. This innovative family of materials comes from combining foam materials (host matrix) with functional phases that lodge within their porous cavities (guest phases). Guest phases do not maintain any chemical or physical union with the host matrix other than mere gravity-caused contact. These materials, together with their manufacturing process and some revealing applications, are patent-protected [3,4] and henceforth referred to as Guefoams (Guest-containing foams) for simplification purposes. Guest phases provide foams different functionalities, so their intrinsic properties no longer limit them. This manuscript covers specific aspects of the manufacturing process of these materials, based on the gas pressure infiltration of a host precursor in preforms conformed by NaCl-coated guest phases. The infiltration process must allow the porosity of the preform to be filled without leading to infiltration of the coating, so that it can later be dissolved in water. For the sake of a specific application, the article involves manufacturing and characterizing aluminum foams containing different proportions of both activated carbon particles and steel spheres as guest phases. This resulted in materials with high adsorption and rapid desorption capabilities due to the previously unattained combination of large specific surface area and magneto-inductive properties in any other cellular material. The manuscript presents a complete study on the adsorption and desorption of butanol, a short-chain hydrocarbon present in paint pigments and resins, in which it is shown that Guefoams contribute to high preconcentration factors and are energy-efficient due to the low power consumption of the inductive-assisted desorption process. The author believes that the

presented ideas, as well as the covered examples and the final discussion on relevant aspects of the applicability of these materials, can inspire the scientific community, especially research groups investigating cellular materials, to design and conceive new multifunctional Guefoams.

2. Guefoams manufacturing process

Guefoams manufacturing process is based on the replication method [5,6], which is conventionally practiced for the production of foams of several natures. In essence, the replication method consists of filling the empty space of a martyr porous preform with a material, usually by means of liquid infiltration, and then eliminating the preform. The original martyr phase is replaced by a porous space that replicates its characteristics. The most widespread replication process involves the use of preforms made up of uniaxial or multiaxial pressure packed NaCl particles, which are liquid infiltrated by a matrix precursor and then removed by water dissolution after precursor solidification. The adaptation of this traditional process to the manufacture of foams with guest phases (Guefoams) lies in the preparation of the particles that comprise the martyr preform. These particles are multi-layered materials where the core is the guest phase, normally with granular geometry, and the outermost material is a continuous NaCl phase covering layer (or other suitable martyr material).

Figure 1a illustrates the manufacturing steps of Guefoam materials that contain one single type of guest phase located in all cavities (Figure 1b). Alternatively, materials with two (or more) guest phases of a different nature, located in a fraction of the available cavities, can also be manufactured (Figure 1c). The main steps are as follows (as shown in Figure 1a in order to manufacture the materials shown in Figures 1b and 1c):

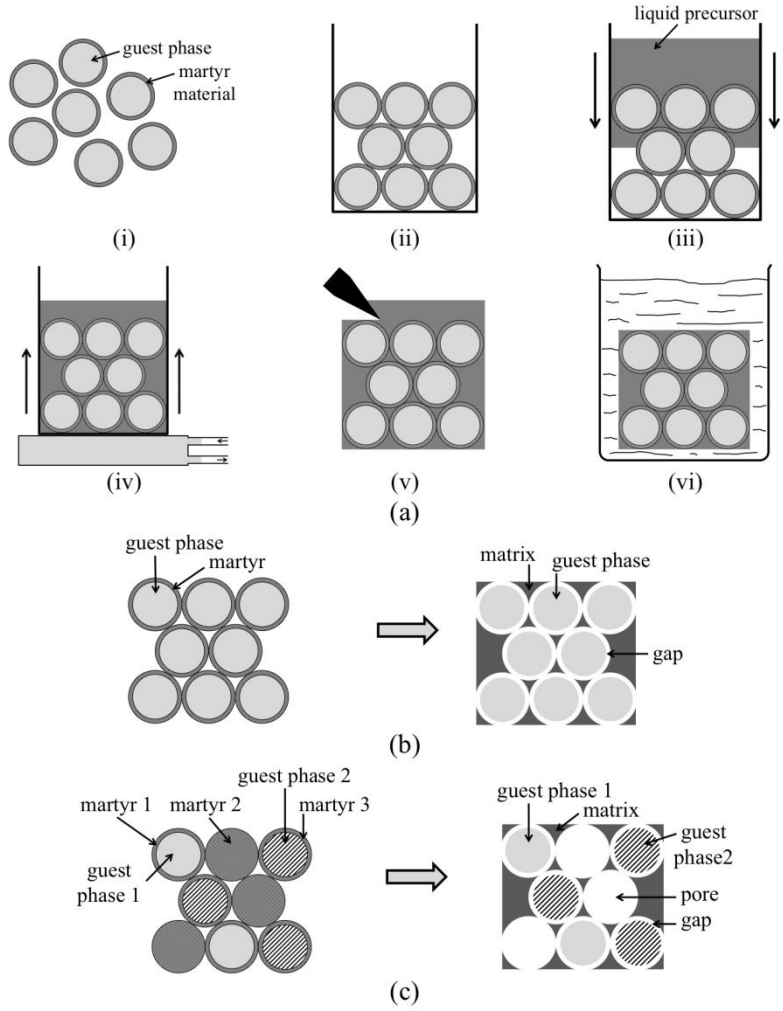

Figure 1 - (a) Manufacturing steps of Guefoams: (i) selection and coating of guest phases; (ii) packaging; (iii) infiltration with liquid precursor; (iv) directional solidification; (v) machining; (vi) removal of martyr material; (b) Guefoam with guest loading of 100% of one type of guest phase; (c) Guefoam with guest loading < 100% of two types of guest phases.

A. Manufacture of the preform.

(i) Selection of one or two-types – eventually more types can be chosen – of guest phases in a finely divided particle or fiber state, and coating them with one or different sacrificial materials;

(ii) Packing of the coated guest phase(s) in a ceramic crucible suitable for infiltration; the packed preform may contain massive particles of a sacrificial

material to generate a fraction of pores containing no guest phases (sacrificial materials of a single nature or of different natures can be used);

B. Infiltration of the packed preform.

(iii) Infiltration of the porous preform with a liquid precursor;

(iv) Solidification of the infiltrating liquid by means of a system allowing directional cooling;

(v) Machining of the structural matrix;

C. Post-infiltration processing.

(vi) Removal of sacrificial material(s) by liquid dissolution or by controlled reaction with a liquid or gas phase.

The resulting material is herein called Guefoam and consists of a host phase that involves locating guest phases in a fraction or in all material cavities without host-guest chemical bonding.

3. Experimental procedures

To manufacture Guefoams, high-purity aluminum (Al 99.999%), purchased from Goodfellow Metals (Cambridge, UK), was used as the liquid infiltrating metal. Two sets of particles were used as guest phases: activated carbon particles of the type Nuchar RGC-30 (Chemical Division of Westvaco, Covington, VA, USA) with a 1 mm of average diameter and low-carbon steel spheres (C: 0.1-0.2%; Mn: 0.6-0.9%; Si: 0.1-0.2%; S: max 0.5%; P: max 0.04%) with average diameters of 1, 1.5, 2 and 3 mm, purchased from Redhill Precision (Lincoln, USA).

Guest phase particles were coated by spray deposition from a 20 wt.% NaCl solution; this concentration produces the least defective coatings when using the coating device described in the patents [3,4]. The NaCl solution was prepared from pure NaCl powder

(99.9%) purchased from AppliChem GmbH (Germany). When required, guest phase-free NaCl spheres were produced by coating with NaCl (by the same spray deposition procedure) raw NaCl particles with an average diameter of about 1mm until a final diameter of approximately 1.4 mm was reached.

Particles (NaCl-coated guest phases of only one type or in combination with other NaCl-coated guest phases and/or NaCl particles) were delicately packed into 18 mm inner diameter graphite crucibles by repeatedly adding a small amount of powder, which was compacted by vibrations [7]. Liquid aluminum infiltrations were performed in a pressure chamber at 720ºC by means of a constant pressurization rate of 0.09 MPa/s and up to variable maximum pressure values, depending on the specific material (see [7] for infiltration details). After metal solidification, the sample was removed from the mold and its surface was ground with SiC paper (400 grit). NaCl coating was dissolved by two different procedures depending on the size of the sample. Large samples (18 mm diameter) were immersed in hot water at 40ºC under magnetic stirring conditions for 6 minutes and then infiltrated with pressurized water following the procedure described in [8-10]. Complete dissolution, as assessed by densitometry, is reached when samples achieve stable weight within approximately 4-5 minutes. The total dissolution time is in consequence about 10-11 minutes. For small samples (8 mm diameter), obtained by cutting larger infiltrated pieces, it was enough to submerge them in hot water at 40ºC under magnetic stirring conditions for a total of 10 minutes.

The basic aspects of the infiltration process were investigated by mercury porosimetry, which was performed in a POREMASTER-60 GT porosimeter (Quantachrome Instruments, Florida, USA) operating at a pressurization rate of 0.09 MPa/s and pressures up to 45 kPa. Materials were characterized by their gas adsorption capacity and magnetic performance. Nitrogen adsorption isotherms were collected at -196ºC in

an Autosorb 6-b equipment of Quantachrome Instruments (Florida, USA) and analyzed within the frame of the standard BET theory [11]. An AMH-DC-TB-S permeameter from the commercial company Laboratorio Elettrofisico (Italy) was used to measure magnetic properties, enabling large samples with cylindrical geometry. Additional permeability and pressure drop measurements were made using a homemade device already presented in [10] and equipped with ±0.001 bar precision manometers at both ends of the sample. Permeability was estimated with injection experiments using water as fluid by monitoring water mass (g) with time (s) on a ±0.1 mg precision balance (Precisa ES320A). The inlet air flow was regulated with a ±0.01 bar precision manometer. Any negligible water mass loss due to evaporation from the collecting container was discarded as the total time of each measurement was <2 min. Using the same device, pressure drop was measured by injecting air as fluid. Air flow was followed with an air flowmeter operating within the 0-30 l/min flow range (Ki Key Instruments, Trevose, UK).

4. Results and discussion

4.1 Infiltration of NaCl-coated particle preforms

The experimental conditions of infiltration herein applied to manufacture Guefoams are isobaric. The selected infiltration pressure therefore determines the metal saturation in the porous preform. The infiltration pressure must be chosen to meet two objectives at the same time: i) it must be sufficient to ensure a minimum metal volume fraction to form a continuous host matrix; and ii) it must not exceed the minimum pressure to initiate NaCl martyr coating infiltration. Compliance with both conditions requires the use of infiltration pressures within a specific interval, which can be determined by liquid metal infiltration studies. Figure 2a shows the results of mercury and aluminum

infiltrations in preforms formed by 1 mm diameter steel spheres coated with approximately 0.5 mm NaCl. Quasi-continuous results for mercury infiltration were obtained at 25ºC with mercury porosimetry. The results corresponding to aluminum were acquired from discrete infiltration experiments at 720ºC and at specific pressures for which metal saturation was determined by densitometry after metal solidification.

The S-shape of the saturation-pressure curves in Figure 2a indicates that infiltration of porous preforms with poorly wetting molten mercury and aluminum metals does not occur in a single step, but rather as a gradual process in which the metal ingress progresses as the applied pressure increases. The process is governed by the well-known semi-empirical Brooks-Corey model [12]:

$$S_{eff} = 1 - S_m = \frac{1 - V_m}{1 - V_r} = \left(\frac{P_b}{P}\right)^{\lambda} \quad (1)$$

where S_{eff} is the effective saturation, defined as the ratio of the volume fraction occupied by the atmosphere ($1-V_m$, where V_m is the metal volume fraction) and the total initial pore volume fraction ($1-V_r$, where V_r is the particle volume fraction). S_m is the metal saturation, P_b is the minimum pressure, also called bubbling pressure, related to the size of the largest pores forming a continuous network of channels in the porous medium, P is the applied pressure and λ is the well-known "pore size distribution index" evaluating the pore size distribution in the porous medium. When Equation (1) holds, plotting $\log(S_{eff})$ *versus* $\log(P)$ must yield straight lines with slope $(-\lambda)$. Figure 2b shows such plots for the data in Figure 2a. Here we can see that, after nonlinear behavior at low pressures, data become linear over most of the pressure range.

Some issues in Figures 2a and 2b are worth discussing. First, the double logarithmic plots present a single slope domain that is identified for mercury and aluminum with values of $\lambda_{Hg} = 4.9$ and $\lambda_{Al} = 5.2$, respectively. These values are fairly high compared to

those obtained for particles with more irregular shape, in line with the values obtained by other researchers for infiltrations of spherical particulate compacts [13]. A constant lambda value for the entire pressure infiltration range indicates a homogeneous pore size distribution of the metal-invaded pore space. At low pressure, metal is expected to invade only the largest interconnected channels of the preform corresponding to the largest voids between particles. Finer channel infiltration, including pores in the NaCl coating (see Figure 2c for details of the porosity inherent in the NaCl coating) occurs at high pressure. Since the present infiltrations are governed by single lambda values, the pressure value at which the infiltration of NaCl coating begins cannot be accurately determined. In order to explore this aspect, coatings were subjected to recrystallization heat treatment (temperature rise for 2 h up to 795ºC, maintenance at this temperature for 2.5 h and, finally, natural cooling down to 25ºC) in which the pore size distribution of the coatings was expected to vary by modifying the crystalline structure of NaCl (Figure 2d). Drainage curves for mercury and aluminum liquid metals were obtained for these treated preforms (Figure 2e). On this occasion, two slope domains were determined from double logarithmic representations (Figure 2f). From the beginning of infiltration to an approximate metal saturation of 0.96 for mercury and 0.94 for aluminum, slopes are identified with values of λ^1_{Hg}= 5.2 for Hg and λ^1_{Al}= 5.2 for Al, in accordance with the values obtained by infiltration of untreated particle preforms. There is a second lower-value slope that governs the last stages of infiltration and corresponds to λ^2_{Hg}= 1.5 and λ^2_{Al}= 1.9 for mercury and aluminum, respectively. At high pressure, a concomitant infiltration of the finest spaces in the preform and pores in the NaCl coating occurs. The lower λ values obtained after recrystallization indicate a more complex pore size distribution of the NaCl coating. Given these results and the fact that the soft recrystallization conditions used here do not significantly alter the average size

of the coarse NaCl crystallites that define the largest pores in the NaCl coating and are first infiltrated, it can be argued that NaCl coating infiltration only starts at pressures for which the preform has been saturated with metal up to approximately 94-96%. For the infiltration with aluminum of the particles considered herein, this is translated into maximum infiltration pressures of approximately 25 kPa (0.25 bar). The first infiltration stages of the NaCl coating may result from the metal invasion of extended defects, such as coverage defaults or cracks (Figures 2g and 2h, respectively). Therefore, the maximum infiltration pressure value can be increased either by NaCl coating procedures which do not produce extended defects and lead to smaller pores or subsequent treatments that cause the pores in the NaCl coating to shrink or close.

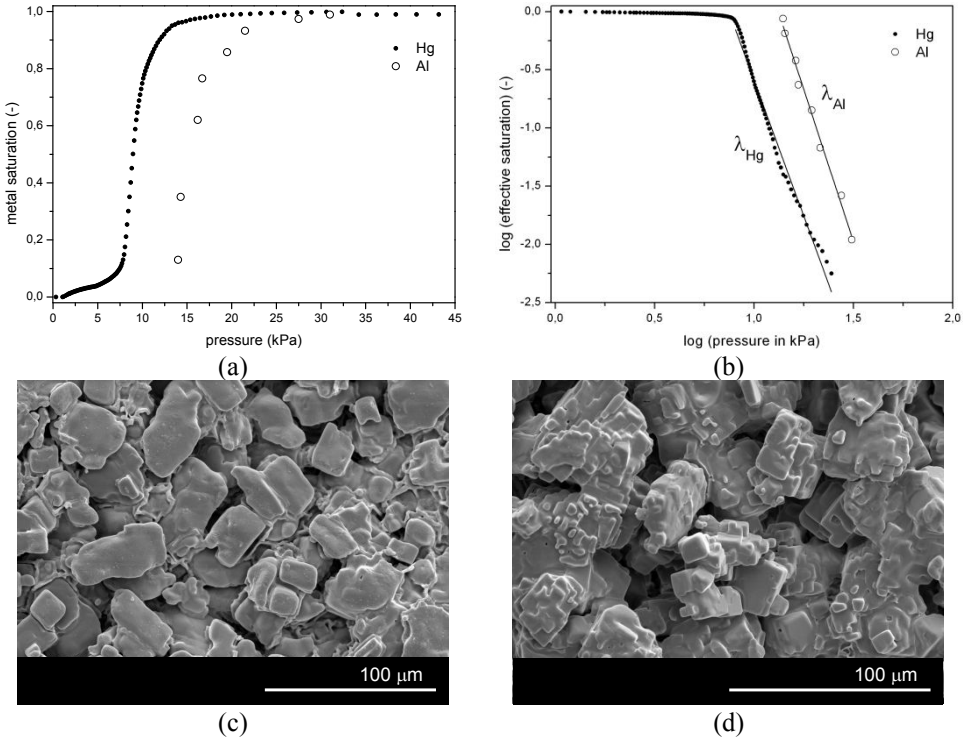

(a) (b)

(c) (d)

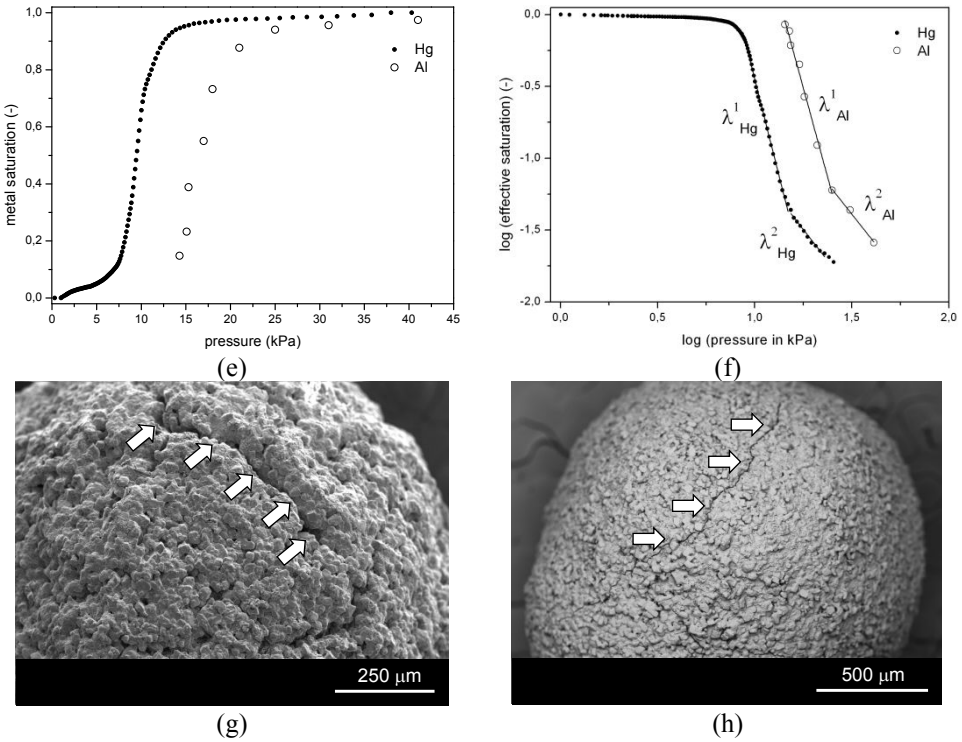

Figure 2. (a) Drainage curves for infiltration of mercury and aluminum in preforms conformed by packing 1 mm spherical steel particles coated with a NaCl layer of approximately 0.5 mm thickness; (b) a double logarithmic representation of the results in (a); (c) and (d) are SEM micrographs corresponding to the NaCl coating and the same coating after thermal treatment for recrystallization, respectively; (e) and (f) correspond to their analogs (a) and (b), respectively, obtained for samples in which the NaCl coating was subjected to recrystallization; (g) and (h) are NaCl coating surface details showing some extended defects (coverage defaults in g and coating cracks in g, in both cases highlighted with arrows). Linear regimes in (b) and (f) were fitted by the equation $\log(S_{eff})=m\cdot\log(P)+n$ *with the following results (R is the linear regression coefficient) – data in (b): m=-4.938, n=4.350, R>0.99 for Hg and m=-5.234, n=5.873, R>0.99 for Al; - data in (f): m=-5.243, n=4.789, R>0.99 for Hg when* $S_m<0.96$*; m=-1.525, n=0.406, R>0.99 for Hg when* $S_m>0.96$*; m=-5.165, n=5.924, R>0.98 for Al when* $S_m<0.94$ *and m=-1.937, n=1.508, R>0.98 for Al when* $S_m>0.94$*).*

4.2 Structure of Guefoams: general structure and features of Al-[C+Fe] Guefoams

Guefoams take the general structure shown in Figure 3a: the host material forms a porous structural matrix and the guest phases are located in all or part of the host cavities, either randomly or in the desired positions. Figure 3a contains two drawings; one is a two-dimensional sketch in which the lines represent interconnecting openings

between pores; the other one is a three-dimensional drawing of a representative material cell containing a cavity-housed guest phase. Since there is a minimal host-guest interaction, limited to mere physical contact caused mainly by gravity force, virtually all guest phase surfaces are functionally active (a particularly important issue in the herein presented case of adsorbent guest phases, such as activated carbon).

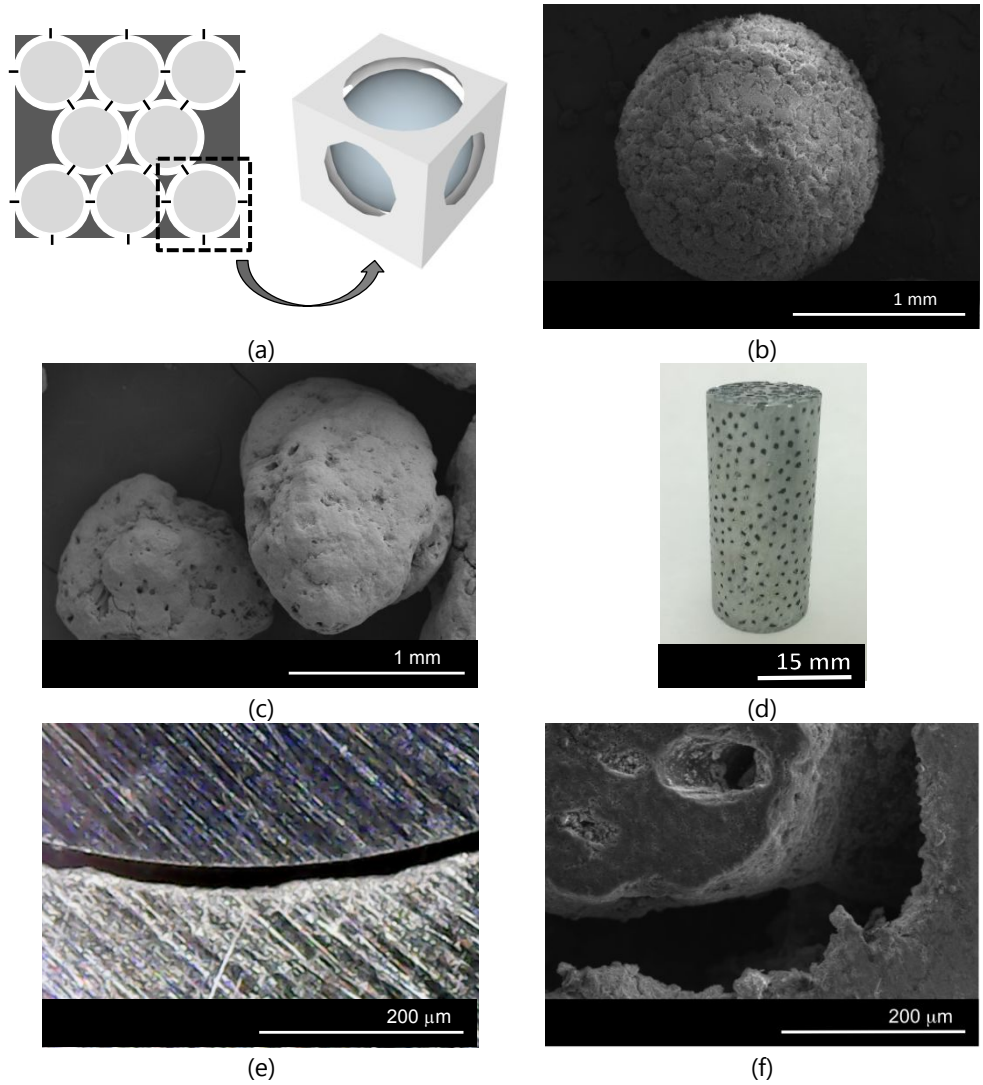

Figure 3 – (a) Schematic diagram of the general structure of Guefoams; (b) SEM micrograph of a NaCl-coated steel sphere; (c) SEM micrograph of NaCl-coated activated carbon particles; (d) photograph of an Al-[C+Fe] Guefoam; and (e-f) optical and SEM micrographs, respectively, showing the space gauge between aluminum skeleton foam and (e) steel sphere and (f) carbon particle.

For the sake of structural characterization, two important parameters are defined:

$$\mathrm{GL}(\%) = \frac{\text{number of pores hosting a guest phase type}}{\text{total number of pores}} \times 100 \qquad (2)$$

$$\mathrm{GO}(\%) = \frac{\text{average volume of a guest specimen}}{\text{average volume of its hosting pore}} \times 100 \qquad (3)$$

where GL and GO refer to *guest loading* and *guest occupation*, respectively. In essence, GL and GO are defined for each type of guest phase contained in the foam material. GL is representative of the percentage of pores that host a certain guest phase. GO refers to the percentage of the volume that a guest phase occupies in the cavity where it is hosted. GL is controlled by the relative proportions of NaCl spheres containing guest phases to those that are guest-free at the moment of preform preparation (see drawing in Figure 1). The thickness of the NaCl coating is the defining parameter for GO (in spherical geometry $GO=(r/R)^3$, where r and R are the average radii of the guest phase and the NaCl-coated guest phase, respectively).

Figures 3b-c show the steel spheres (1.5 mm average diameter) and activated carbon particles, respectively after NaCl coating, used in the manufacture of Al-[C+Fe] Guefoams; that is, aluminum foams with different proportions of guest phases of both steel spheres and activated carbon particles. These materials were fabricated at an infiltration pressure of 22 kPa, a value low enough not to infiltrate the fine pores of the NaCl martyr coating (other examples of selective preform infiltrations can be found in [14,15], where infiltration pressures were properly selected to avoid infiltration of the internal structure of NaCl consolidated particles). Figure 3d depicts a photograph of a 17 mm diameter and 32 mm long Guefoam sample in which all pores contain guest phases, one half containing activated carbon particles and the other half containing steel spheres. Figures 3e-f are optical and SEM micrographs, respectively, showing in detail the remaining space between the host and guest phases. This gap can be filled with a

static or moving fluid because the lack of host-guest chemical bonding causes the interconnecting windows between pores to remain open.

4.3 Magnetic and adsorbent properties of Al-[C], Al-[Fe] and Al-[C+Fe] Guefoams

Table 1 gathers the properties of the Guefoam samples prepared in this work, where the host phase is aluminum, and the nature of the guest phases (carbon particles, steel spheres or combinations of both) and their guest loadings (GL) were varied. Samples are referred to as Al-[C], Al-[Fe] or Al-[C+Fe] Guefoams, where C and Fe indicate the activated carbon particles and steel spheres, respectively.

Table 1 – Characteristics and properties of manufactured Al foam (Al-0 sample) and Guefoams of aluminum as the host phase and activated carbon particles (C), steel spheres (Fe) of 1.5 mm average diameter, or mixture of both, as guest phases (samples Al-[C], Al-[Fe] and Al-[C+Fe], respectively). GL refers to guest loading and GO to guest occupation. S_{BET} (m^2/cm^3 or m^2/g) is the area obtained by nitrogen adsorption at -196ºC; M_s, M_r and H_c are saturation magnetization (emu/g), remanent magnetization (emu/g) and magnetic coercitivity (Oe), respectively.

Sample code	GL (%) (±1)		GO (%) (±1)		Volume fraction (±0.02)				Main property measured				
									S_{BET}		M_s	M_r	H_c
	C	Fe	C	Fe	Al	C	Fe	pores	(m^2/cm^3)	(m^2/g)			
Al-0	0	0	-	-	0.37	0.00	0.00	0.63	0.11	0.11	-	-	-
Al-[C]_1	25		58			0.09	0.00	0.54	101	91.5	-	-	-
Al-[C]_2	50					0.18	0.00	0.44	202	173	-	-	-
Al-[C]_3	100					0.36	0.00	0.27	409	312	-	-	-
Al-[Fe]_1	0	10	-	87		0.00	0.05	0.58	0.12	0.08	48.0	0.08	8.28
Al-[Fe]_2		45				0.00	0.24	0.39	0.12	0.04	109	0.51	9.96
Al-[Fe]_3		70				0.00	0.38	0.25	0.12	0.03	128	0.79	10.32
Al-[Fe]_4		100				0.00	0.54	0.09	0.16	0.03	132	1.10	10.45
Al-[C+Fe]_1	10	10	58			0.04	0.05	0.54	38.4	25.9	47.5	0.09	7.87
Al-[C+Fe]_2	50	10				0.18	0.05	0.40	201	126	44.2	0.08	7.70
Al-[C+Fe]_3	75	10				0.27	0.05	0.31	308	185	41.6	0.09	7.72
Al-[C+Fe]_4	10	50				0.04	0.27	0.32	42.3	13.3	112	0.54	9.19
Al-[C+Fe]_5	10	75				0.04	0.41	0.19	40.5	9.54	128	0.76	9.52
Al-[C+Fe]_6	50	50				0.18	0.27	0.18	204	62.0	106	0.47	9.43

In all cases, the volume fraction of aluminum is 0.37. This value agrees, given that S_{eff}≈0.95 at 22 kPa, with an effective packing of 0.61 for the volume fraction of the

NaCl-coated guest particles measured when preparing the martyr preform. Raw (NaCl-uncoated) activated carbon and steel particles attain packing volume fractions of 0.56 and 0.61, respectively, by following the same packing method. This indicates that the NaCl coating partially spheroidizes the irregular surface of the activated carbon particles and increases their packing efficiency. At first glance, we can observe that the Al-0 sample (sample manufactured by infiltration of NaCl spheres containing no guest phase) exhibits a small surface area of approximately 0.11 m^2/cm^3, which is consistent with the low values reported in previous findings for replicated carbon foams [8]. When guest phases are present in all or part of the pores, the functionalities provided by each appear rather independently, so that the properties of the materials derive from the individual contributions of the present guest phases through their respective volume fractions. This is certainly due to the net physical separation of guest phases and the absence of chemical bonding with the host matrix.

Figure 4 displays the magnetization curves and the nitrogen adsorption capacity of some samples in Table 1. The magnetization curves shown in Figure 4a are consistent with the magnitude scale measured for composites with variable ferromagnetic spheres loads [16-19]. Figure 4b is a magnification of Figure 4a for low magnetic fields in which the characteristic hysteresis loops of ferromagnetic materials are distinguished. The curves corresponding to Figure 4c are defined as Type II adsorption curves. The main differences between the curves are primarily due to the amount of adsorbent in each case. Figure 4d shows that the volume-specific surface areas (S_{BET} in m^2/m^3) scale linearly with the activated carbon volume fraction. This is not the case for mass-specific surface areas, S_{BET} in m^2/g, as steel particles do not contribute to a substantial area rise but significantly increase the final density of the material.

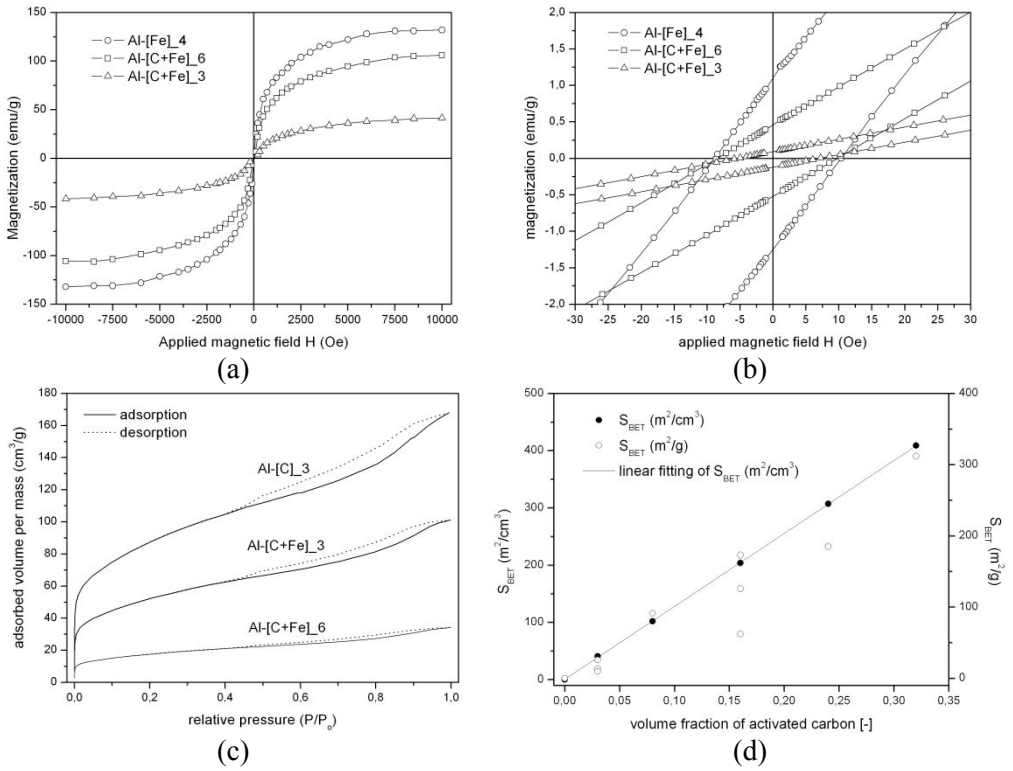

Figure 4 – (a) Magnetization curves for some Guefoams containing steel as guest phase; (b) details of the magnetization curves of (a) at low applied magnetic fields to determine magnetic coercitivity H_c; (c) nitrogen adsorption isotherms (volume per mass unit versus relative pressure P/P_o where P_o is the saturation pressure) for some Guefoams containing activated carbon as guest phase; (d) the correlation between the specific surfaces measured by the BET method from curves in (c) versus the volume fraction of activated carbon; the straight line fitting the S_{BET} (m^2/cm^3) data has a regression coefficient >0.99.

4.4 Application of Al-[C+Fe] Guefoams in portable VOCs preconcentration devices

The Al-[C+Fe] Guefoams manufactured here may, among other applications, be used to trap and preconcentrate contaminants such as short-chain hydrocarbons (phenol, ethanol, butanol, etc.) normally present in synthetic paint pigments and resins. The magnetic properties of some prepared Guefoams make them suitable for rapid adhesion to magnetized surfaces of structural architectures and can also help them to be recovered from fluid storage tanks where they may have been submerged. Magnetic properties also allow these materials to be rapidly heated by magnetic induction [20,21]

to efficiently desorb trapped substances. The device shown in Figure 5a was designed to test the performance of these materials in real applications. This device gathers portable characteristics due to its small dimensions and its 12V-battery autonomous electrical supply. It consists mainly of a metal case covering the foam material (with dimensions 45 mm long and 8 mm diameter), which has a winding copper varnished wire around it. This set is attached to an induction generator powered by the 12V AC battery and a control plate containing a main switch, a maximum electrical current limiter and a frequency selector. Figure 5b shows the heating speeds of different samples under magnetic induction conditions in the device referred to for two powers (28W and 62W) and in a 350W conventional electrical resistance furnace. It is clear from the findings that magnetic induction generates higher heating speeds at much lower powers. In addition, the heating speed of Al-[C+Fe] Guefoams (exemplified by sample Al-[C+Fe]_6), which depends on frequency and induction power, is linear over the time scales used here and much higher than that of conventional aluminum foam (Al-0 sample) (Figure 5b).

As proof of concept, butanol was adsorbed into the Al-[C+Fe]_6 sample by passing through it nitrogen carrier gas flowing at room temperature and 450 ml/min with 0.3 mmol/l butanol inlet concentration C_o. Butanol adsorption rate was followed with time by the analysis of butanol concentrations (C) at the sample outlet measured by a micro-chromatograph (MTI P200H). The corresponding breakthrough curve (a C/C_o versus time representation) is shown in Figure 5c. Samples were then extracted from the device for further characterization and subjected to a differential thermal gravimetry (DTG) analysis using a thermo balance (Setaram TGA-92) coupled with a magnetic induction system, which enables adjustable sample heating rates by operating at different

induction powers and a fixed frequency of 200 kHz. A helium gas flow of 12 ml/min was used during desorption.

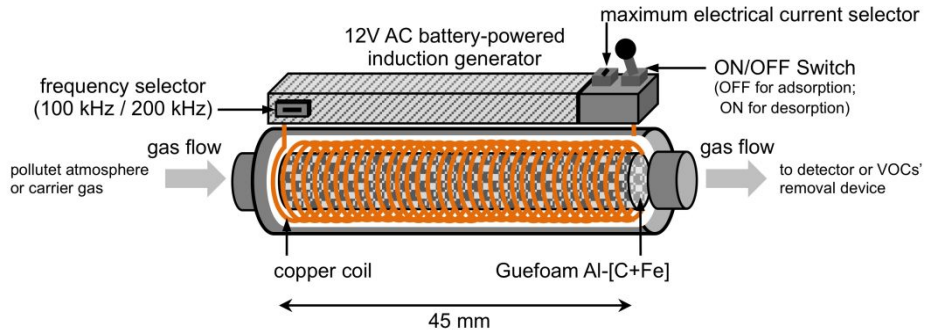

(a)

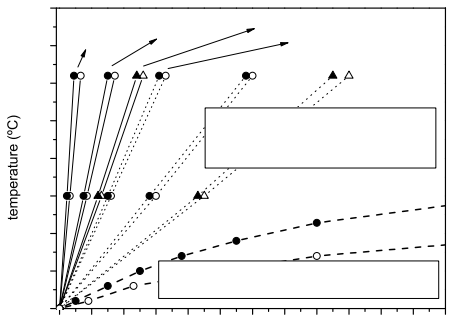

(b)

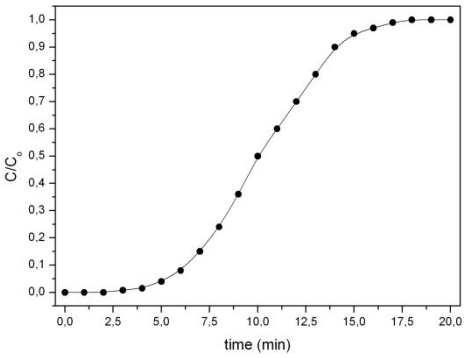

(c)

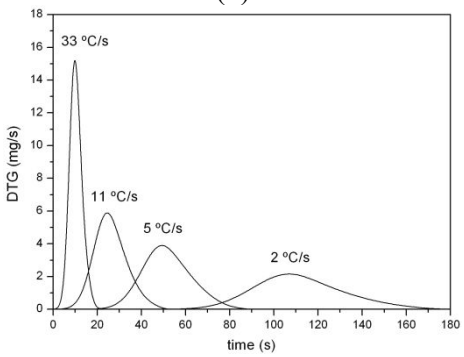

(d)

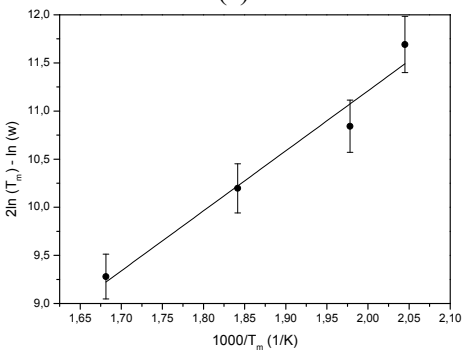

(e)

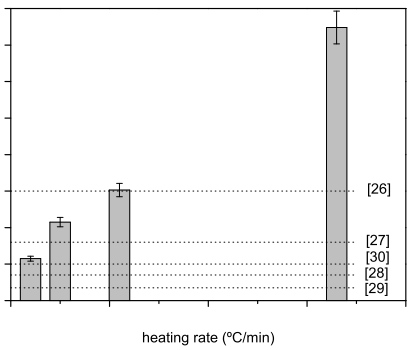

(f)

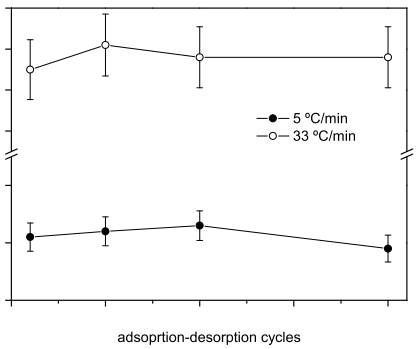

(g)

Figure 5 – (a) Portable device for preconcentration and management of VOCs by adsorption and rapid desorption through magnetic induction heating; (b) heating rate curves - surface (R=4 mm) and core temperatures (R=0 mm) versus time - for samples Al-0 and Al-[C+Fe]_6 with dimensions of 45 mm long and 8 mm diameter under magnetic induction heating at frequencies of 100 kHz and 200 kHz and powers of 28W and 62W; for comparison purposes, the heating rate for the Al-[C+Fe]_6 sample under conventional electrical heating is included; (c) the breakthrough curve for butanol adsorption for the Al-[C+Fe]_6 sample; (d) the differential thermal desorption (DTG) curves for butanol desorption at different heating rates for the Al-[C+Fe]_6 sample; and (e) the plot of $2\ln(T_m)-\ln(w)$ versus $1000/T_m$, where T_m and w are the maximum peak temperature in DTG and the heating rate, respectively - the straight line fitting the data is $2\ln(T_m)-\ln(w)=6236\cdot\ln(w)-1.262$, with a regression coefficient >0.96; (f) the concentration enrichment factor values attained with the Al-[C+Fe]_6 sample at different heating rates together with some values achieved in bibliography for VOCs solid-gas extraction systems using adsorption-desorption cycles; (g) the enrichment factor values obtained in several adsorption-desorption cycles.

The DTG results (Figure 5d) confirmed that the butanol desorption process from the activated carbon contained in Al-[C+Fe]_6 Guefoam was easily controlled by the heating rate which, in turn, was determined by the magnetic induction capacity of the sample. From the data obtained, the enthalpy for butanol desorption from the herein used RGC-30 activated carbon was derived by the linear transformation proposed by Cvetanovic and Amenomiya [22] and generalized in [23] for different experimental conditions. It consists of plotting $2\ln(T_m)-\ln(w)$ *versus* $(1/T_m)$, where T_m and w are the temperature corresponding to the maximum desorption rate (peak temperature in DTG) and the heating rate, respectively (Figure 5e). The value obtained for butanol desorption from the RGC-30 activated carbon was 51.8 kJ/mol, which is in close agreement with other values obtained for activated carbons generated by carbonizing wood of different natures (coconut wood was the raw material employed for RGC-30 production). This value was higher than butanol vaporization heat (approximately 43.7 kJ/mol [22]),

suggesting that strongly endothermic processes occur during the desorption process, as noted in previous works [24,25]. Integrating the curves in Figure 5d results in desorbed butanol quantities at all heating speeds of approximately 104 mg, corresponding to desorption percentages above 99% of the butanol quantities previously adsorbed.

Figure 5f shows the butanol concentration enrichment factor (EF) achieved for various heating speeds. EF is a parameter widely used in analytical processes defined as the ratio of the concentration of analyte (butanol) in the desorbed gas to the concentration of analyte in the carrier gas prior to adsorption in the pre-concentrator device. Such concentrations were determined with an MTI P200H microchromatograph. The major enrichment factor corresponds to 33ºC/min, for which EF=150 is achieved. This value is well above other values attained in the bibliography for preconcentration of VOCs in solid-gas extraction systems using adsorption-desorption cycles, among which we highlight the value of EF=60 achieved in the enrichment of butanol obtained by fermentation [26] or the value of EF=32 attained in porphyrin-modified carbon nanotube systems [27]. The EF results obtained for 1-butanol using an odor-measuring system employing a mass sensitive sensor array based on quartz crystal microbalance (QMB) [28] or the values attained with metal-organic frameworks for hazardous trace gases [29] remain well below these values. One of the most interesting works published on this topic is the microwave-assisted desorption of VOCs on activated carbon [30], for which a preconcentration factor of only about 20 is deduced. Figure 5g presents the concentration enrichment factor obtained for several adsorption-desorption cycles. The values can be verified to remain approximately constant at intervals up to 20 cycles.

5. Relevant aspects of the applicability of Guefoams as chemical preconcentrators

Guefoams are essentially open-pore foams and, as such, owe their greatest functionality to their interconnected porous space, which allows fluids to pass through them. The presence of guest phases may significantly alter the intrinsic fluid-dynamic characteristics of these materials, such as their permeability or fluid pressure drop. To explore this, aluminum foams and Guefoams of aluminum as host phase and steel particles as guest phases were manufactured. Steel spheres were 2 or 3 mm in diameter, each covered by NaCl until reaching a final 3.5 mm diameter. Two infiltration pressures of 15 kPa and 22 kPa were explored. The characteristics and properties of the manufactured specimens can be seen in Table 2.

Table 2 – Characteristics and properties of the manufactured Al foams (Al-x-y sample) and Guefoams of aluminum as the host phase and steel spheres (Fe) as guest phases (Al-[Fe]_x-y samples). x and y in the sample code refer to the steel spheres diameter (in mm) and infiltration pressure (in kPa), respectively (two nominal average diameters - 2 and 3 mm - and two infiltration pressures - 15 and 22 kPa - were used). The average pore size of each sample was 3.5 mm. GL refers to guest loading and GO to guest occupation. K is permeability in m² and ΔP is pressure drop in kPa/m, measured at different airflow velocities v (in m/s).

Sample code	GL (%) (±1)	GO (%) (±1)	Volume fraction (±0.02)			Main property measured			
	Fe	Fe	Al	Fe	pores	K	ΔP/ΔL		
							v = 0.01	v = 0.025	v = 0.05
Al-0-15	0	0	0.20	0.00	0.80	5.56×10^{-11}	4.10	13.0	32.0
Al-0-22			0.37	0.00	0.63	2.79×10^{-11}	8.46	27.2	67.1
Al-[Fe]_2-15	100	16	0.21	0.09	0.70	1.78×10^{-11}	14.9	31.0	78.9
Al-[Fe]_2-22			0.37	0.10	0.53	1.06×10^{-11}	20.0	59.1	141
Al-[Fe]_3-15		53	0.19	0.32	0.49	1.05×10^{-11}	19.9	56.6	129
Al-[Fe]_3-22			0.37	0.33	0.30	3.35×10^{-12}	65.0	172	383

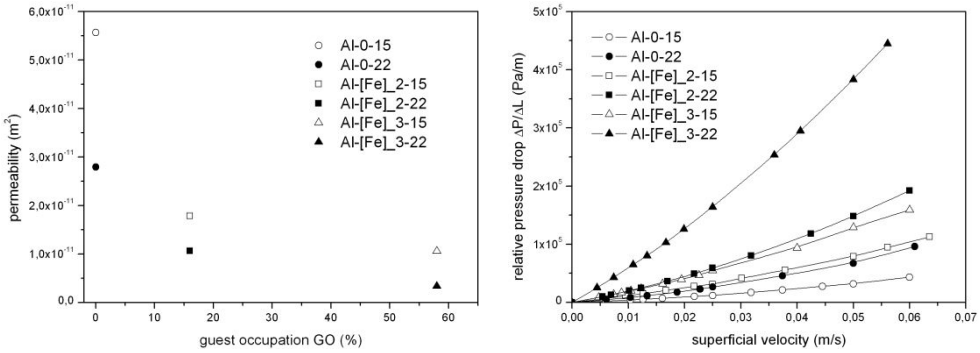

(a) (b)

Figure 6. (a) Permeability versus guest occupation (GO in %) and (b) the relative pressure drop versus superficial velocity for samples in Table 2.

Figure 6a depicts sample permeability values in Table 2 as a function of guest occupation. This graph shows that permeability decreases as infiltration pressure and guest occupation increases. Dependence on infiltration pressure is easily understood as higher infiltration pressures generate higher metal saturations in the NaCl particulate preform (see Equation 1). Consequently, narrower interconnection channels between pores are generated after NaCl particle dissolution. Such channels determine the permeability of these open-pore media in conventional foams (see experimental results and analytical models in [31]). Permeability in Guefoams is even lower than in their analogous conventional foams due to the lower volume of interconnected porosity through which flow can pass. This latter effect can also be qualitatively deduced from the models described in [31]. As a result of the drop in permeability due to the presence of guest phases, an increase in the pressure drop required to make fluid pass through the porous space of Guefoams is expected. This behavior is seen in Figure 6b, where pressure drop is plotted according to airflow velocity.

Permeability and pressure drop in foam materials are determining factors for their use as chemical preconcentrators. The presence of guest phases generates some resistance to fluid passage that must be taken into account. Indeed, far from being a disadvantage, it

can become a clear advantage since a decrease in permeability has been shown to increase the fluid dwelling time within the porous foam skeleton. This has resulted in better heat transfer between circulating fluid and solid phases [32], which can improve the homogeneity of the temperature distribution in the material, thereby favoring the thermal desorption process. At present, an exhaustive characterization of permeability, pressure drop and heat transfer coefficient is being carried out on Guefoams of different characteristics.

6. Conclusions

In summary, this manuscript presents a new family of multifunctional materials consisting of host open-cell foam materials with cavities locating functional guest specimens and their use for preconcentration and management of VOCs. Lack of host-guest chemical interactions ensures pore connectivity to enable fluid transport while maintaining guest phase functionalities. Adequate host and guest compositions may bring new property combinations uncovered by any foam material and definitely open the way to challenge new technological frontiers. For each particular system, the infiltration process followed in the manufacture of these materials must be studied thoroughly because the host phase precursor must not infiltrate the NaCl coatings so that they can later be dissolved in water. In the present case, the maximum infiltration pressure was determined at 25 kPa, a pressure from which the infiltration of NaCl coatings made by spray coating begins. As proof of concept, the article entails the manufacture, characterization and testing of aluminum foams with carbon and steel guest phases (Al-[C+Fe] Guefoams). These materials are highly capable of adsorbing volatile organic compounds (VOCs) such as butanol (the compound studied in this manuscript), and can desorb them by fast and low-power magnetic induction heating to

become excellent and energy-efficient preconcentrators and managers of VOCs. Based on their significance for the applicability of these materials, certain characteristic parameters such as permeability or pressure drop on fluid passage are discussed. It was found that the permeability decreased with the percentage of guest occupation, while the pressure drop increased, two characteristics that could enhance the heat exchange between the circulating fluid and the solid phases, thereby enabling a faster and more efficient desorption process. Essentially, the new Guefoam family materials feature extended properties hitherto unattained in conventional open-pore foams and offer tremendous potential to impact new system performance in current and future applications requiring advanced multifunctional materials.

Acknowledgement

The author acknowledges financial support from the Spanish "Agencia Estatal de Investigación" (AEI) and European Union (FEDER funds) through grant MAT2016-77742-C2-2-P.

References

[1] Ferreira, A.D.B.L.; Nóvoa, P.R.O.; Marques, A.T. Multifunctional Material Systems : A state-of-the-art review. Compos. Struct. 2016, 151, 3–35.

[2] Salonitis, K.; Pandremenos, J.; Paralikas, J.; Chryssolouris, G. Multifunctional materials: Engineering applications and processing challenges. Int. J. Adv. Manuf. Technol. 2010, 49 (5–8), 803–826.

[3] Molina-Jordá, J.M. Materiales espumados de poro interconectado con fases huésped, procedimiento para la preparación de dichos materiales y usos de los mismos. Spanish Patent P201730890, 2017.

[4] Molina-Jordá, J.M. Materiales espumados de poro interconectado con fases

huésped, procedimiento para la preparación de dichos materiales y usos de los mismos. PCT Patent PCT/ES2018/070474, 2018.

[5] Kuchek, H.A. Method of making porous metallic article. United States Patent 3236706, 1964.

[6] Carlson, N.G. Cast porous metal. United States Patent 3210166, 1967.

[7] Molina, J.M.; Saravanan, R.A.; Arpón, R.; García-Cordovilla, C.; Louis, E.; Narciso, J. Pressure infiltration of liquid aluminium into packed SiC particulate with a bimodal size distribution, Acta Mater. 2002, 50, 247–257.

[8] Molina-Jordá, J.M. Mesophase pitch-derived graphite foams with selective distribution of TiC nanoparticles for catalytic applications. Carbon 2016, 103, 5-8.

[9] Molina-Jordá, J.M. Multi-scale design of novel materials for emerging challenges in active thermal management: Open-pore magnesium-diamond composite foams with nano-engineered interfaces. Compos. Part A Appl. Sci. Manuf. 2018, 105, 265-273.

[10] Maiorano, L.P.; Molina, J.M. Challenging thermal management by incorporation of graphite into aluminium foams. Mater. Des. 2018, 158, 160–171.

[11] Brunauer, E.T.S.; Deming, L.S.; Deming, W.E. On a theory of the van der Waals adsorption of gases. J. Am. Ceram. Soc. 1940, 62(7), 1723–1732.

[12] Brooks, R.H.; Corey, A.T. Hydraulic properties of porous media. Hydrology papers. Colorado State University 1964.

[13] Samani, S.; Geistlinger, H. Simulation of Channelized Gas Flow Pattern in Heterogeneous Porous Media : A Feasibility Study of Continuum Simulation at Bench Scale. Vadose Zone J. 2019 18:180144.

[14] Mortensen, A.; Goodall, R. Porous metal article and method of producing a porous metallic article. United States Patent US 8.151.860 B2, 2011.

[15] Goodall, R.; Mortensen, A. Microcellular aluminium? - Child's play!. Adv. Eng. Mater. 2007, 9, 951-954.

[16] Antonel, P.S.; Berhó, F.M.; Jorge, G; Molina, F.V. Magnetic composites of $CoFe_2O_4$ nanoparticles in a poly(aniline) matrix: Enhancement of remanence ratio and coercivity. Synth. Met. 2015, 199, 292–302.

[17] Kramarenko, E.Y.; Chertovich, A.V.; Stepanov, G.V.; Semisalova, A.S.; Makarova, L.A.; Perov, N.S.; Khokhlov, A.R. Magnetic and viscoelastic response of elastomers with hard magnetic filler. Smart Mater. Struct. 2015, 24, 1-11.

[18] Zhao, H.; Weng, L.; Cui, W.W.; Zhang, X.R.; Xu, H.Y.; Liu, L.Z. In situ anchor

of magnetic Fe_3O_4 nanoparticles onto natural maifanite as efficient heterogeneous Fenton-like catalyst. Front. Mater. Sci. 2016, 10, 300-309.

[19] Borgohain, C.; Acharyya, K.; Sarma, S.; Senapati, K.K.; Sarma, K.C.; Phukan, P. A new aluminum-based metal matrix composite reinforced with cobalt ferrite magnetic nanoparticle. J. Mater. Sci. 2013, 48, 162-171.

[20] Bayerl, T.; Schledjewski, R.; Mitschang, P. Induction heating of thermoplastic materials by particulate heating promoters. Polym. Polym. Compos. 2012, 20, 333-342.

[21] Bae, D.H.; Shin, P.; Kwak, S.; Moon, M.; Shon, M.; Oh, S.; Kim, G. Heating behavior of ferromagnetic Fe particle-embedded thermoplastic polyurethane adhesive film by induction heating. J. Ind. Eng. Chem. 2015, 30, 92-97.

[22] Cvetanović, R.J.; Amenomiya, Y. Application of a temperature-programmed desorption technique to catalyst studies. Catal. Rev. 1972, 6, 21-48.

[23] Jolly, J.P.; Perrard, A. Determination of the heat of adsorption of ammonia on zeolites from temperature-programmed desorption experiments. Langmuir 2001, 17, 1538-1542.

[24] Popescu, M.; Jolly, J.P.; Carré, J.; Danatoiu, C. Dynamical adsorption and temperature-programmed desorption of VOCs (toluene, butyl acetate and butanol) on activated carbons. Carbon 2003, 41, 739-748.

[25] Senf, L.; Frank, H. Thermal desorption of organic pollutants enriched on activated carbon. J. Chromatogr. 1990, 520, 131-135.

[26] Raganati, F.; Procentese, A.; Olivieri, G.; Russo, M.E.; Salatino, P.; Marzocchella, A. Bio-butanol recovery by adsorption/desorption processes. Sep. Purif. Technol. 2019, 235, 116145.

[27] Lvova, L.; Mastroianni, M.; Pomarico, G.; Santonico, M.; Pennazza, G.; Di Natale, C.; Paolesse, R.; D'Amico, A. Carbon nanotubes modified with porphyrin units for gaseous phase chemical sensing. Sensors Actuat B-Chem. 2012, 170, 163-171.

[28] Yuwono, A.S.; Niess, J.; Hamacher, T.; Boeker, P.; Lammers, P.S. Odour measuring system using a mass sensitive sensor array and its performance improvement. 2nd World Engineering Congress, July 2002, pp. 1–3.

[29] Woellner, M.; Hausdorf, S.; Klein, N.; Mueller, P.; Smith, M.W.; Kaskel, S. Adsorption and Detection of Hazardous Trace Gases by Metal – Organic Frameworks. Adv. Mater. 2018, 30, 1-27.

[30] Fayaz, M.; Shariaty, P.; Atkinson, J.D.; Hashisho, Z.; Phillips, J.H.; Anderson, J.E.; Nichols, M. Using microwave heating to improve the desorption efficiency of high

molecular weight VOC from beaded activated carbon. Envir. Sci. Technol. 2015, 49(7), 4536-4542.

[31] Despois, J.-F.; Mortensen, A. Permeability of open-pore microcellular materials. Acta Mater. 2005, 53, 1381-1388.

[32] Zaragoza, G.; Goodall, R. Metal foams with graded pore size for heat transfer applications. Adv. Eng. Mater. 2013, 15(3), 123-128.

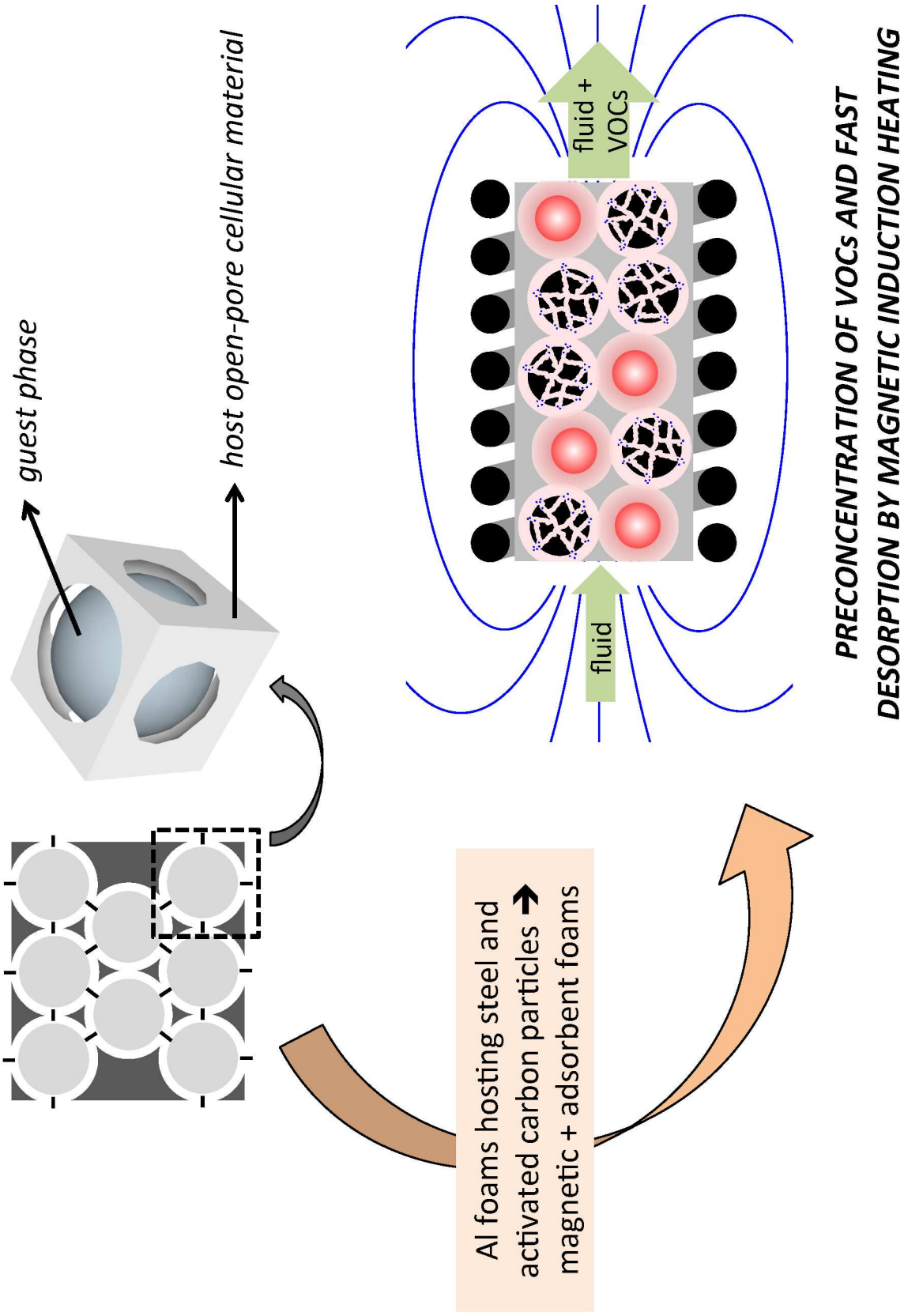
guest phase
host open-pore cellular material
fluid + VOCs
fluid
PRECONCENTRATION OF VOCs AND FAST DESORPTION BY MAGNETIC INDUCTION HEATING
Al foams hosting steel and activated carbon particles ➔ magnetic + adsorbent foams